Eurographics/ IEEE-VGTC Symposium on Visualization (2006)
Thomas Ertl, Ken Joy, and Beatriz Santos (Editors)

# Robust Surface Detection for Variance Comparison and Dimensional Measurement

C. Heinzl[†], R. Klingesberger[†], J. Kastner[†] and E. Gröller[‡]

[†]Upper Austrian University of Applied Sciences, Stelzhammerstrasse 23, A-4600 Wels, Austria
[‡]Vienna University of Technology, Institute of Computer Graphics and Algorithms, Karlsplatz 13, A-1040 Vienna, Austria

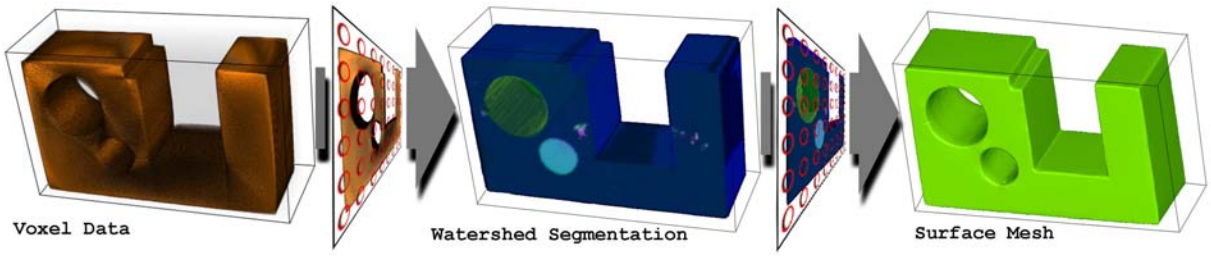


**Figure 1:** *Homogeneous industrial work piece segmentation based on 3D watershed and constrained elastic-surface nets*

**Abstract**

*This paper describes a robust method for creating surface models from volume datasets with distorted density values due to artefacts and noise. Application scenario for the presented work is variance comparison and dimensional measurement of homogeneous industrial components in industrial high resolution 3D computed tomography (3D-CT). We propose a pipeline which uses common 3D image processing filters for pre-processing and segmentation of 3D-CT datasets in order to create the surface model. In particular, a pre-filtering step reduces noise and artefacts without blurring edges in the dataset. A watershed filter is applied on the gradient information of the smoothed data to create a binary dataset. Finally the surface model is constructed, using constrained elastic-surface nets to generate a smooth but feature preserving mesh of a binary volume. The major contribution of this paper is the development of the specific processing pipeline for homogeneous industrial components to handle large resolution data of industrial CT scanners. The pipeline is crucial for the following visual inspection of deviations.*

Categories and Subject Descriptors (according to ACM CCS): I.3.8 [Computer Graphics]: Applications

## 1. Introduction

In modern engineering the complexity of industrial products is continuously increasing while development times have to be as short as possible. To meet the short development periods in rapid product development, the requirements in terms of quality assurance are very high.

Variance comparison is a common means of quality assurance. Its primary usage is to compare the measured geometry of a specimen with reference geometry data. The aim of this process is to get an overview of the deviation at each location of the specimen. In dimensional measurement primarily crucial distances are of interest, in order to compare a component's dimensions with the specifications of a computer

[†] {c.heinzl|r.klingesberger|j.kastner}@fh-wels.at
[‡] groeller@cg.tuwien.ac.at

aided design (CAD) model. Especially the automotive industry is interested in variance comparison and dimensional measurement to verify the quality of prototypes and samples. For example in the case of an oil filter housing, shape distortion may occur while cooling down the melted material. So it is essential to adapt the production process to guarantee specified tolerances and finally to reach an optimal shape of the component. Other application areas can be found in aeronautics and consumer industry.

Common surface-based methods like coordinate measuring or optical methods cannot measure internal features. For providing the full geometric information, the importance and applicability of 3D-CT is increasing. 3D-CT is a radiographic method for Non Destructive Testing (NDT) to locate and size volumetric details in three dimensions. A 3D-CT scanner generates a series of X-ray attenuation measurements, which are used to produce a 3D grid of greyvalues directly corresponding to the spatial density information [KSBS04]. The major difference between medical CTs and industrial CTs is that medical CTs produce a calibrated dataset. Compared to conventional radiography, 3D-CTs are more prone to artefacts like noise-induced streaks, aliasing, beam-hardening, partial volume or scattered radiation effects [Hsi03]. Typically in 3D-CT systems with cone beam X-ray sources, the quality of the datasets is affected by the specimen's material, its geometry, the penetration lengths and after all the positioning of the specimen in the ray.

For common surface-model extraction-tasks in industrial applications, usually a single isovalue is specified to distinguish between material and air (see [Vol04]). A polygonal mesh is extracted along the selected isovalue using a surface creation algorithm. For example the marching cubes algorithm creates triangle models of constant density surfaces from 3D volume data [LC87]. However, in datasets with distorted density values, the classification of material with a single, global threshold is difficult and sometimes impossible. Artefacts modify the greyvalues in areas of complex geometry and large penetration lengths. So for a global isovalue, structures are added due to artefacts in certain areas, while in other regions the structure is thinned and even holes appear. In Figure 2 these cases are depicted showing a 3D view of a complex die-cast component with a global isovalue. The blue detail image a) still shows big holes emerging in the structure, while in the red detail image b) volume is already added.

As CT datasets always contain artefacts to a certain amount, this paper concentrates on designing a new method, that locally adapts contours (see Figure 1). The greyvalues of the voxel dataset are taken as "ground truth" trying to extract as much information as possible. Our major aim is to create a pipeline which is robust with respect to artefacts. The pipeline has to be applicable in variance comparison and dimensional measurement tasks. Furthermore, it has to be practicable in terms of data-processing speed and quality.

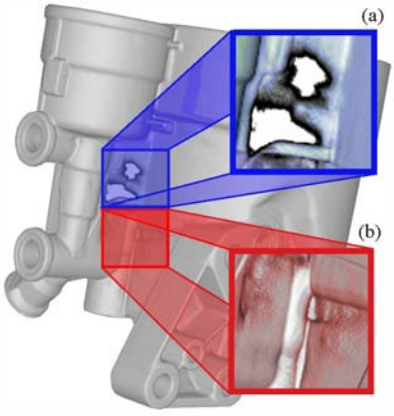


**Figure 2:** *CT dataset of an industrial filter housing, large penetration lengths and complex geometry result in heavy artefacts. (a) thinning and holes, (b) additional volume through thickening*

## 2. Related work

There are several methods in the area of industrial computed tomography, that try to improve on artefact-affected data. Generally they can be grouped into two sets: either the dataset is enhanced by artefact reduction (see [Kas05]) so that a single threshold is sufficient. Or the dataset is considered as "ground truth" and the best possible surface is extracted.

Steinbeiss [Ste05] developed an algorithm that locally adapts a global threshold setting. First, an initial isosurface is generated using a suitable global threshold. Along the direction of the surface normal of a considered vertex, the algorithm creates a greyvalue profile. The vertex location is then moved to the position with maximal gradient magnitude. In a further refinement, the local grey level of material and background is determined. The vertex location is adjusted to the position of the mean of local material and background grey values. The method is sensitive to noise of real CT-scans, which Steinbeiss tries to reduce by considering neighbouring greyvalue profiles. Due to averaging of vertex positions the algorithm modifies the surface and it cannot distinguish between noise and small details.

Whitaker et al. [WB98] introduced an approach that directly operates on voxel data. In this approach the intermediate step of converting data to another representation is not necessary. The basic idea is to consider the zero level-set of a volume as a deformable surface. The surface is then deformed in order to minimize the mean curvature on the surface. The method by Whitaker et al. does not contain any data pre-filtering to reduce artefacts. Furthermore it does not generate a surface mesh, which is necessary in common industrial reverse engineering tools like Geomagic Qualify.

Bischoff and Kobbelt [BK02] have presented algorithms

on isosurface-topology simplification and isosurface reconstruction with topology control. They use a priori knowledge about the topology of the input data to eliminate the topological artefacts that arise from the noise. Let us assume that the desired topology and an approximating shape are known beforehand. An initial triangle mesh is then adjusted to match a given shape by applying topology-preserving operations. Bischoff and Kobbelt's approach is not suitable for our application scenario because topolocial information is not known a priori.

Gibson [Gib98] proposed a method which extracts the surface from binary data. This algorithm detects surface vertices depending on the eight greyvalues of a volume cell. After connecting the surface vertices, the surface net is relaxed minimizing an energy measure. The original segmentation is maintained by a constraint forcing each vertex to stay within its original volume cell. Triangulation of the surface points generates the final surface model. Gibson's method assumes binary-segmented data as input. For our application it has to be extended with a mechanism for artefact reduction and for binarization. In the presented pipeline model these extensions are introduced.

## 3. Homogeneous industrial workpiece segmentation

In order to extract as much information of a dataset as possible, the use of fully three dimensional pre-processing algorithms is essential. This guarantees, that no information about the third dimension gets lost. An information loss might happen if one executes a segmentation algorithm just on two dimensional slice images. In the following subsections all components of the proposed pipeline (see Figure 3) are discussed in detail:

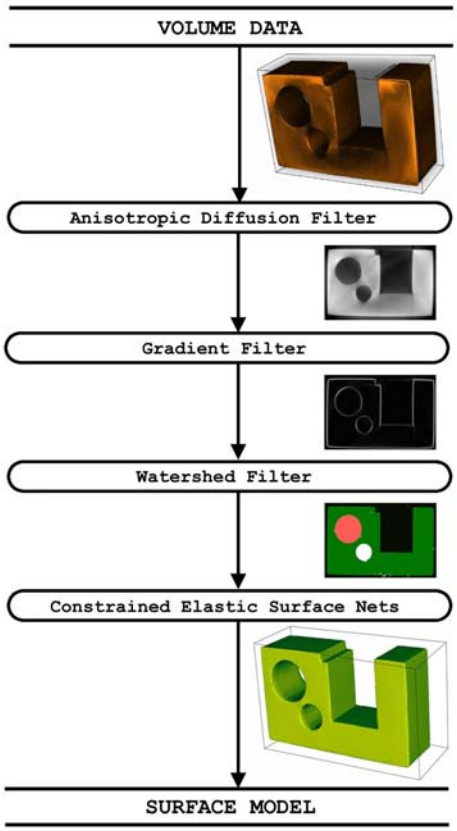


**Figure 3:** *Workpiece segmentation and surface extraction of homogeneous industrial components; Input: volume dataset with distorted density values, Output: Surface mesh*

### 3.1. Anisotropic-Diffusion Filter

As 3D-CT scans are affected to a certain degree by ambient noise, post-processing steps are subjected to uncertainty. To reduce ambient noise as well as smaller artefacts, a smoothing algorithm has to be applied. Standard isotropic diffusion methods, for example gauss filtering, blur the input image with a filter kernel applied on each voxel. As each voxel is blurred, boundaries are moved. Therefore these methods are unacceptable for geometry-comparison tasks. In order to provide the segmentation with smooth input data without blurred edges, an anisotropic-diffusion filter is applied.

Anisotropic-diffusion methods are used to reduce noise in images while preserving specific image features [PM90]. Perona and Malik's method calculates multi-scale descriptions of images. If an image $U(\mathbf{x})$ is embedded in a higher dimensional function of derived images $U(\mathbf{x},t)$ then this higher dimensional function represents the solution of the heat diffusion equation,

$$\frac{dU(\mathbf{x},t)}{dt} = \nabla \cdot C \nabla U(\mathbf{x},t) \qquad (1)$$

with the constraint of a constant conductance coefficient $C$ and the initial condition $U(\mathbf{x},0) = U(\mathbf{x})$ representing the original image. If $C$ is extended to a function of $\mathbf{x}$, the solution of the heat equation will be

$$\frac{dU(\mathbf{x},t)}{dt} = C(\mathbf{x})\Delta U(\mathbf{x},t) + \nabla C(\mathbf{x}) \nabla U(\mathbf{x},t) \qquad (2)$$

A variable conductance term $C$ can now modify the way the diffusion process takes place. Typically, $C$ is chosen as a function of image features. This allows to selectively preserve or remove features by anisotropically varying the diffusion strength. Specifying $C$ as a nonnegative monotonically descending function as in

$$C(\mathbf{x}) = e^{-\left(\frac{\|\nabla U(\mathbf{x})\|}{K}\right)^2}, \qquad K = const \qquad (3)$$

will force the diffusion to mainly take place in homogeneous interior regions and it will not affect the boundary regions [IS03].

Applying an anisotropic-diffusion filter, the quality of the datasets can be significantly improved. Scattered radiation

effects are removed without blurring edges, which is essential for surface detection. Figure 4 shows a cross section before and after pre-filtering the dataset.

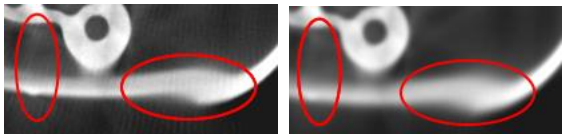

(a) (b)

**Figure 4:** *Anisotropic-Diffusion Filter, axial cross section through a filter housing, (a) scattered radiation artefacts throughout the material, (b) after anisotropic diffusion filtering small artefacts are removed; some artefacts are marked by ellipses*

### 3.2. Gradient Filter and Watershed Filter

After pre-filtering, the greyvalues of material areas still vary to a certain extent due to beam hardening, scattered radiation, and other artefacts. Using varying greyvalues as input to the segmentation task results in misclassification of artefact-affected areas. In the presented application scenario, the gradient magnitudes of the pre-filtered data are calculated. This is achieved by computing the directional derivative at each location of the dataset using a first-order derivative operator.

For the segmentation task, a simple segmentation algorithm is not robust in terms of greyvalue deviations. Region growing for example, implicitly uses a global threshold. Therefore it produces similar thickening and thinning structures like global thresholding. In order to build up a binary volume by grouping regions with similar greyvalues, watershed segmentation is used. Watershed segmentation is a low-level image analysis algorithm producing a hierarchy of segmented and labelled regions from a scalar-valued input. In geography, a watershed region is bordered by the ridges of neighbouring catchment basins. In image processing, images are depicted as height functions: A catchment basin is defined around each local minimum of the height function, such that each of its points is connected with the minimum by a descending path [VS91]. To avoid oversegmentation, a flooding level is defined. The height function is flooded up to a certain level to decrease the number of extracted regions. Shallow segments with lower levels than the flood level will merge, eroding boundaries of adjacent regions.

For the binarization task, Šrámek et al. [ŠD02] proposed a classification method, which is based on watershed hierarchies. In our approach we use a much simpler, faster and in most of the cases sufficient way for binarization. The mean greyvalues of the remaining regions are calculated and classified by a global threshold.

### 3.3. Constrained Elastic-Surface Nets

After the binary volume has been extracted, a surface mesh is generated. A marching cubes algorithm applied on a binary volume creates a jagged surface. This jagged surface accurately represents the binary volume but not the original surface of the specimen.

Gibson [Gib98] proposes constrained elastic-surface nets, a method to create a smooth surface model from binary datasets which still preserves fine details. Gibson's algorithm consists of four steps: First, vertices of the surface are identified using volume cells. All volume cells intersected by the surface are identified. If every cell corner has the same binary value, then the volume cell has to be completely inside or completely outside the segmented object. Otherwise a surface cell has been found. In this case a surface vertex $p[i]$ is initialized by placing the vertex in the centre of the volume cell. Then, surface vertices are linked and the neighbourhood for each vertex is determined. Assuming only face connected neighbour volume-cells, each vertex in the volume can have a maximum of six linked neighbour volume cells. In the relaxation step, the position of each surface vertex is modified according to the number of neighbours $N(i)$:

$$\hat{p}[i] = \frac{1}{\#\{N(i)\}} \sum_{j \in N(i)} p[j] \tag{4}$$

An energy measure calculated from the edges controls the smoothing process. The energy is computed as the sum of the squared lengths of all edges in the surface net. To retain thin structures, a constraint is defined which forces every vertex to stay within its original volume cell. After several iterations of the smoothing procedure, the energy quickly reaches a minimum level where the surface turns out to be smoothest. At a higher number of iterations, the energy level converges at a slightly higher value and edges become sharper. In the final step the surface is being triangulated.

## 4. Results and discussion

In this section results are discussed when applying our pipeline on homogeneous reference objects as well as on a real industrial die-cast component. All CT scans were performed on a HWM RayScan 250E system with a 225 kV microfocus X-ray tube. Reference measurements were performed on a Zeiss C400 coordinate measuring machine with an absolute accuracy of +/-2$\mu$m. Our demo application containing the presented pipeline was implemented in Visual C++ using ITK [IS03] libraries for image processing and VTK [SML04] libraries for visualization. All 3D views are rendered using raycasting.

### 4.1. Reference objects

Workpiece one is a regular aluminium test part (Figure 5) developed by Kasperl [Kas05]. It has two cylindrical drill holes

with different diameters and a rectangular milling. This object produces severe scattered radiation artefacts due to the different penetration lengths at a relatively high material thickness. Figure 5 shows a CT scan of workpiece one with strong artefacts changing the geometry of the smaller drill hole. Settings of this measurement: 810 projection images, voltage 200kV, current 620$\mu$A, integration time 500ms. To reduce artefacts, the X-ray beam is prefiltered using physical pre-filtering plates of 0.1mm Pb and 0.15mm Cu, in order to minimize low energetic radiation. The resulting 16Bit dataset is 339*525*169 voxels in size with a voxelsize of 200$\mu$m.

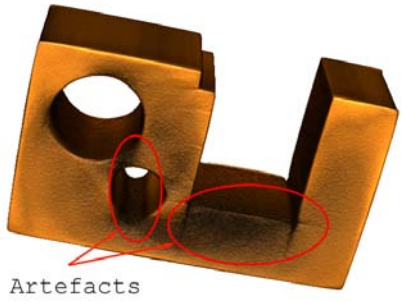


**Figure 5:** *CT-scan of workpiece one. This reference object creates severe scattered radiation and beam hardening artefacts in the area of the drill holes and the rectangular milling. In the areas affected by artefacts the geometry is modified (see smaller drill hole)*

Workpiece two is an aluminium step cylinder (Figure 6). The step cylinder consists of 5 concentric rings with increasing outer diameters and a drill hole along the longitudinal axis. This object is used as reference for geometric and dimensional measurement in 3D-CT, because it allows to classify different inner and outer diameters at different wall thicknesses. Due to the increasing wall thickness in the lower rings, artefacts affect the dataset so that it is difficult to distinguish between material and air in the drill hole. With this object the limitations of a 3D-CT concerning geometric and dimensional measurement can be shown. Settings of this measurement: 720 projection images, at 210kV, 1000$\mu$A, 500ms integration time, 1mm Cu pre-filtering resulting in a 16bit dataset of 561*559*436 voxels with a voxelsize of 236$\mu$m.
Workpiece three is a real industrial component (Figure 2). The complex filter housing generates artefacts in the area of the bridge between the two joining parts. Measuring this object, severe artefacts appeared in the central area (see Figure 2). While in detail image a) thinning and holes are shown in detail image b) structures are added through thickening. The dataset was measured with a voxelsize of 252$\mu$m using 810 projection images at 210kV, 830$\mu$A, 500ms integration time and 1mm Cu pre-filtering. These settings resulted in a dataset of over 1GB in size. Our developed demo application cannot handle this amount of data yet. Therefore a representative subgrid of 529*771*100 voxels was taken, which covers the artefact-affected area.

(a)

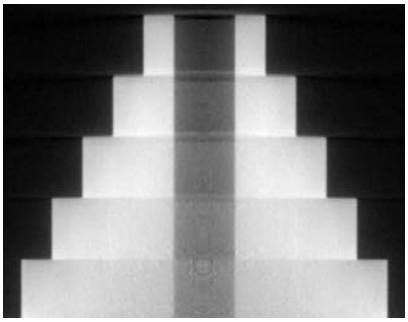

(b)

**Figure 6:** *CT scan of workpiece two, Oblique view (a) shows the reference object which is used for geometric and dimensional measurement tasks. Along the horizontal axis the outer ring diameters and wall thicknesses increase, while the inner ring diameters remain constant. Small variations of the data values result in a fine texturing in the result images. The sagital cross-section (b) shows increasing artefacts in the centre drill hole when wall thicknesses are increasing*

### 4.2. Tuning the pipeline

To produce a usable surface model, the parameter settings of the filters are crucial. The anisotropic-diffusion filter is used to support the watershed segmentation in producing fewer and bigger regions. Excluding this filter would lead to oversegmentation or misclassifications in artefact-affected areas. We used general settings of 5 iterations at a conductance of 50. For workpieces with severe artefacts, we increased the number of iterations to 7 and the conductance to 75. The anisotropic diffusion filter takes 65-70% of the whole processing time. Therefore the number of iterations is a major

factor in the overall processing time.
Applying the watershed segmentation, the flooding threshold influences merging of small regions with similar greyvalues. On the one hand oversegmentation can be significantly reduced using a higher threshold. On the other hand, regions of air, whose greyvalues are slightly below the surrounding material greylevel, will be misclassified. Especially in the lower rings of workpiece two, this effect can be found. So the flooding level has to be set individually for each dataset. Generally, the processing time of the watershed segmentation is related to the smoothness of the dataset. A dataset, which is not pre-filtered, either increases the overall processing time disproportionately or forces the program to crash due to memory limitations. Our findings are that for all three datasets, the processing time of the watershed segmentation was 25-30% of the overall processing time.
For the constrained elastic-surface nets, the same number of iterations is used for creating the surface of all three workpieces. The energy level reaches a minimum after 8 to 10 iterations. After 20-30 iterations the edges are further sharpened which improves the overall accuracy. Therefore the number of iterations is fixed to 30 iterations for all datasets. Increasing the number of iterations is not crucial for the overall processing time because the constrained elastic-surface nets take only 5% of the processing time.

A general approach to tune the pipeline consists of the following steps: Firstly, the parameters of the diffusion filter have to be adjusted. To increase diffusion, the number of iterations is increased. The conductance controls the sensitivity of the conductance term: the lower the conductance value, the more strongly the diffusion equation preserves image features. Secondly for the watershed segmentation the flooding level has to be set. To avoid unintentional region merges the flooding level has to be set well above air greylevel but below the lowest material grey level. For the binary classification of the remaining regions, the mean greyvalue of the material regions has to be found.

### 4.3. Analysis

In the case of workpiece one, severe artefacts distort the greyvalues of the dataset due to high material thicknesses (see Figure 7). In order to reduce oversegmentation and misdetections, pre-filtering is increased. The desired result of a fully connected binary volume without artefacts could be achieved with the disadvantage of a higher overall processing time. As depicted in Figure 8 the presented method is able to remedy the erroneously modified geometry in the area of the drill holes. Furthermore the scattered radiation effects in the area of the rectangular milling could be significantly reduced. To verify the exactness of lengths, a surface representation of workpiece two was extracted using our pipeline. In this surface representation, five cross sections in the middle of each ring were specified. For each of these cross sections the inner and outer diameters are calculated using a circle fit. In Figure 9 conventional surface extraction with the best possible isovalue is compared to the output of the presented pipeline with the CAD model as reference. In order to double-check the calculated distances due to our pipeline, the diameters are measured with a coordinate measuring machine (CMM). Furthermore the distances are compared to the best isovalue setting. Results are shown in table 1. Compared with the CMM a mean deviation of 9$\mu$m for the outer diameters and 57$\mu$m for the inner diameters could be reached. Applying our pipeline on workpiece three, the geometry could be extracted without creating holes in the area of severe artefacts. In this area, where global threshold-

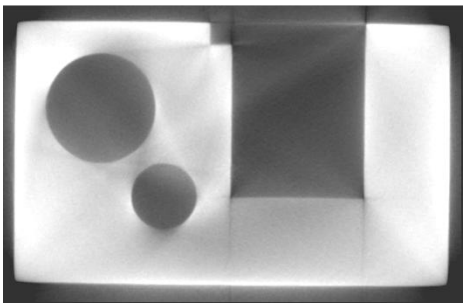

**Figure 7:** *Axial cross section of workpiece one. Severe scattered radiation and beam hardening are present. Greyvalues of the drill holes and the rectangular milling are elevated*

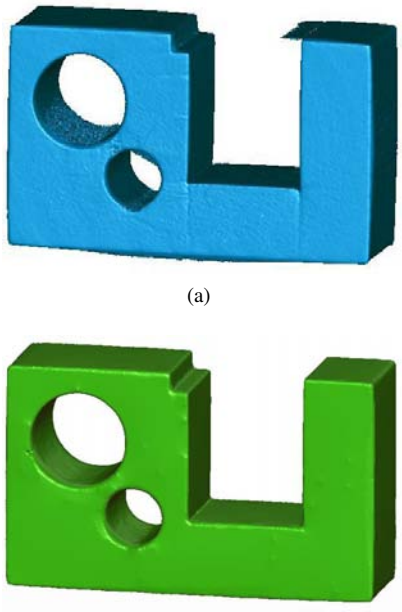

(a) (b)

**Figure 8:** *Surface model of workpiece one: (a) best isosurface, (b) presented method: geometric modifications, thinning and thickening artefacts are successfully removed*

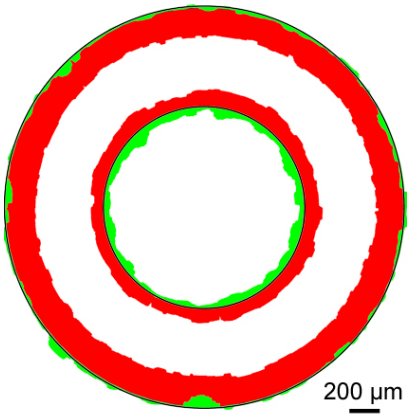


(a)

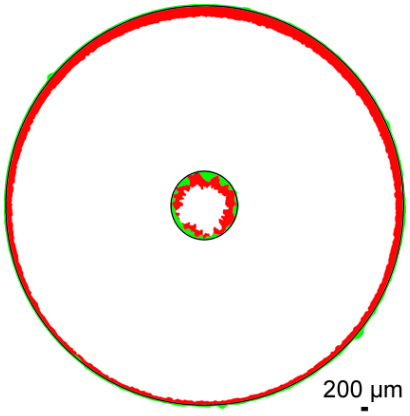


(b)

**Figure 9:** *2D variance comparison of the three resulting surface models. Axial cross section in the middle of (a) first and (b) last ring. The CAD model was taken as reference (black). The best global isovalue of workpiece two is depicted in red and the output of the presented pipeline in green. Variations of the inner and outer contours are depicted 15 times scaled. Mind the different scales: inner circles of both figures have the same size*

| # | CAD[mm] | CMM[mm] | ISO[mm] | PIPE[mm] |
|---|---|---|---|---|
| 1 | 20.00 | 19.985 | 20.202 | 19.932 |
| | 40.00 | 40.014 | 39.667 | 40.015 |
| 2 | 20.00 | 19.985 | 19.736 | 19.920 |
| | 60.00 | 60.017 | 59.695 | 59.996 |
| 3 | 20.00 | 19.985 | 19.487 | 19.923 |
| | 80.00 | 80.014 | 79.620 | 80.003 |
| 4 | 20.00 | 19.985 | 19.372 | 19.924 |
| | 100.00 | 100.014 | 99.632 | 100.005 |
| 5 | 20.00 | 19.985 | 19.574 | 19.938 |
| | 120.00 | 120.011 | 119.693 | 120.009 |

**Table 1:** *Dimensional measurement results of inner and outer diameters for each ring of workpiece two, Dimensions of CAD model (CAD), coordinate measuring machine (CMM), best global isovalue (ISO), and the output of the presented pipeline (PIPE) are depicted*

ing produces holes, a mean deviation of +/-36$\mu$m between constructed surface and CAD model is achieved.

For variance comparison, three visualization methods are applied. A common method for variance comparison is colour coding. Each position of the reference object is coded with a colour corresponding to the local deviation. In this visualization, a scalar is mapped onto a 3D object representation. The direction of the deviation vector is not considered. Figure 10a depicts a colour coded visualization generated using Geomagic Qualify. If an arrow is placed at each vertex pointing in the direction of the corresponding deviation vector, a three dimensional deviation information can be included (Figure 10b). In addition the vector glyphs are colour coded and scaled according to the absolute value of the deviation. Due to scaling the glyphs this representation allows to quickly identify areas of great deviations. As glyphs represent the deviation vector, a better representation of the test object can be generated in relation to the reference object. Furthermore the directional information illustrates the alignment between reference and test object. A third visualization method maps cylinders to the surface model (Figure 10c).

The overall processing times were measured on an Athlon 64 4000+ system with 1GB RAM. On this system the processing times for extracting a surface are 4:58 minutes for workpiece one, 10:23 minutes for workpiece two and 4:44 minutes for workpiece three.

## 5. Summary and conclusions

This paper describes a new pipeline for industrial workpiece segmentation allowing automated and effective variance comparison. The presented method offers the possibility to extract reproducible surface models from artefact distorted volumes. The presented pipeline model is to a certain extent robust concerning common artefact types, which is of great importance for variance comparison and dimensional measurement tasks. Furthermore the accuracy and the applicability on industrial components has been discussed. A major aim of our future work is to add support for multimaterial workpieces. In the area of visualization, the glyph based visualization methods will be enhanced and new visualization methods will be evaluated.

## 6. Acknowledgements

The presented work has been funded by the FH-Plus project “Zerstörungsfreie und In-situ-Charakterisierung von Werk-

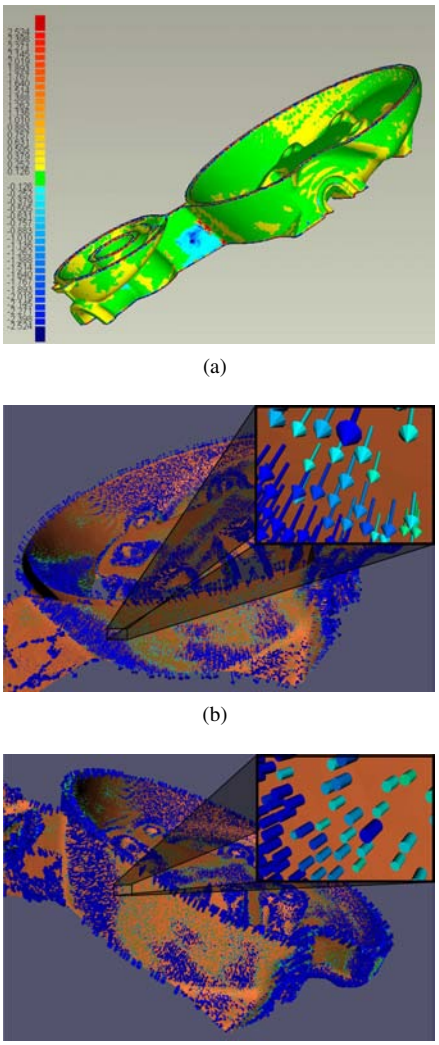

(a) (b) (c)

**Figure 10:** *Variance comparison for workpiece three (representative sub grid) between best isovalue vs. pipeline. Colour-coded visualization (a), glyph-based visualization using arrows (b), and cylinders (c)*

stücken und Materialien unter besonderer Berücksichtigung von Brennstoffzellen" (see http://www.fh-wels.at) of the Austrian Research Promotion Agency (FFG). Furthermore this work is partly supported by the PVG project, Austrian Science Fund (FWF) grant no P18547-N13.
Thanks to Gruber&Kaja Druckguss for providing the filter housing, Matej Mlejnek and the visgroup of the Vienna University of Technology, Institute of Computer Graphics and Algorithms, for support in designing the pipeline, Milos Šrámek for suggestions and ideas concerning 3D watershed and CT group of the Upper Austrian University of Applied Sciences for fruitful discussions and CT measurements.

## References

[BK02] BISCHOFF S., KOBBELT L.: Isosurface reconstruction with topology control. In *Pacific Conference on Computer Graphics and Applications* (2002), pp. 246–255.

[Gib98] GIBSON S. F.: Constrained elastic surface nets: generating smooth surfaces from binary segmented data. In *Lecture Notes In Computer Science* (1998), vol. 1496, pp. 888–898.

[Hsi03] HSIEH J.: *Computed Tomography : Principles, Design, Artifacts and Recent Advances*. SPIE-The International Society for Optical Engineering, 2003.

[IS03] IBANEZ L., SCHROEDER W.: *The ITK Software Guide*. Kitware, Inc., 2003.

[Kas05] KASPERL S.: *Qualitätsverbesserungen durch referenzfreie Artefaktreduzierung und Oberflächennormierung in der industriellen 3D-Computertomographie*. PhD thesis, Technische Fakultät der Universität Erlangen Nürnberg, 2005.

[KSBS04] KASTNER J., SCHLOTTHAUER E., BURGHOLZER P., STIFTER D.: Comparison of x-ray computed tomography and optical coherence tomography for characterisation of glass-fibre polymer matrix composites. In *Proceedings of WCNDT* (2004), pp. 71–79.

[LC87] LORENSEN W., CLINE H.: Marching cubes: A high resolution 3D surface construction algorithm. In *ACM SIGGRAPH Computer Graphics* (1987), vol. 21, pp. 163–169.

[PM90] PERONA P., MALIK J.: Scale-space and edge detection using anisotropic diffusion. In *IEEE Transactions on Pattern Analysis and Machine Intelligence* (1990), vol. 12, pp. 629–639.

[ŠD02] ŠRÁMEK M., DIMITROV L. I.: Segmentation of tomographic data by hierarchical watershed transform. *Journal of Medical Informatics and Technologies*, 3 (2002), 161–169.

[SML04] SCHROEDER W., MARTIN K., LORENSEN B.: *The Visualization Toolkit*. Kitware, Inc., 2004.

[Ste05] STEINBEISS H.: *Dimensionelles Messen mit Mikro-Computertomographie*. PhD thesis, Technische Universität München, 2005.

[Vol04] VOLUMEGRAPHICS: *VG Studio Max 1.2 - User's Manual*. 2004.

[VS91] VINCENT L., SOILLE P.: Watersheds in digital spaces: An efficient algorithm based on immersion simulations. In *IEEE Transactions on Pattern Analysis and Machine Intelligence* (1991), vol. 13.

[WB98] WHITAKER R. T., BREEN D. E.: Level-set models for the deformation of solid objects. In *The third international workshop on implicit surfaces* (1998), pp. 19–35.